Therapeutic effect of silibinin on vanadium-induced chronic lung injury in mice

Hobin Im
Kyungpook National University
Eungyung Kim
Kyungpook National University
Hong Ju Kwon
Kyungpook National University
Hyeonjin Kim
Kyungpook National University
Na Eun Cho
Kyungpook National University
Jiwon Ko
Kyungpook National University
Yonghun Sung
Daegu-Gyeongbuk Medical Innovation Foundation
Soyeon Jang
Kyungpook National University
Sung-Hyun Kim
Korea Polytechnic College
Eun Jung Lee
Korea Polytechnic College
Duhak Yoon
Kyungpook National University
Woo-Sung Kwon
Kyungpook National University
Zae Young Ryoo
Kyungpook National University
Jun Koo Yi
Gyeongsangbukdo Livestock Research institute
Myoung Ok Kim (ok4325@knu.ac.kr)
Kyungpook National University

Article

Keywords: V2O5, Silibinin, Lung injury, NF-kB, NLRP3, MAPK signaling pathway

Posted Date: May 3rd, 2022

DOI: https://doi.org/10.21203/rs.3.rs-1548568/v1

Abstract

Background: Silibinin has shown therapeutic effects in various inflammatory and cancer models. However, the therapeutic effect and underlying mechanism in V2O5-induced pulmonary inflammation, which consists of particulate matter and metal components, have not been identified. We examined the potential anti-inflammatory activity and underlying mechanism of silibinin in a vanadium-induced lung injury model.

Results: Silibinin treatment resulted in a significant restoration of cell viability and reduced infiltration of inflammatory cells in a histological analysis. In addition, silibinin significantly reduced the expression of the pro-inflammatory cytokines, TNF-α, IL-6, and IL-1β. Furthermore, silibinin reduced inflammation by down-regulating the MAPK and NF-kB signaling pathways and the NLRP3 inflammasome. Treatment with silibinin significantly reduced the NLRP3 expression levels in lung tissue.

Conclusion: These results indicate that silibinin exhibits anti-inflammatory effects in V2O5-induced inflammatory mice.

Introduction

Air pollution is a serious environmental problem that is caused by the advancement of industrialization and urbanization[1–3]. Over the past few decades, studies have shown an association between air pollution and a variety of lung diseases including lung cancer, asthma, and chronic obstructive pulmonary disease[4]. Particulate matter (PM), a type of air pollution, affects not only the lungs, but also other organs [5–7]. PM is classified according to size: PM10 is a particle less than 10 μm, whereas PM2.5 is considered fine particulate matter. After exposure, PM2.5 penetrates into the bronchial tube and infiltrate the fine bronchial tree and alveoli [8]. There are many sources of PM, such as road traffic, industrial emissions, construction sites, fuel combustion, soil resuspension, and secondary emissions [9,10]. PM contains sulfate, nitrate, heavy metal (vanadium pentoxide, lead, iron, cadmium), and polycyclic aromatic hydrocarbons. Studies suggest that human exposure to PM less than 2.5 μm in diameter damages respiratory, cardiovascular, and reproductive functions [11–15]. Metal, vanadium pentoxide (V2O5), volcanic ash, and fossil fuels are some of the PM2.5 components floating around in atmosphere. Also, chronic exposure to V2O5 may cause serious lung toxicity [16].

According to previous studies, V2O5 induces oxidative stress by increasing the level of reactive oxygen species (ROS) [17]. Pulmonary edema and inflammation also occur in the lungs of workers exposed to vanadium [14,18]. In a study of mice exposed to V2O5 for an extended time, chronic lung inflammation, lung cancer, reproductive disorders, and vascular inflammation were observed [19–22]. The lungs are the most susceptible organ to damage from particle exposure. Therefore, lung inflammation induced by V2O5, which is one of the metal components in PM, is an important area of investigation [23].

The MAPK and NF-kB signaling pathways are very important during the inflammatory process [24–27]. Increasing ROS induces oxidative stress and activation of NF-kB increases the secretion of various inflammatory cytokines, including TNF-α, IL-6, and IL-1β [28]. Subsequently, a pulmonary inflammatory reaction occurs through the infiltration of lung tissue by inflammatory cells [29]. In addition, activation of the NLRP3 inflammasome resulting from increased ROS causes inflammation by releasing IL-1β following caspase-1 cleavage [30].

Several molecules, such as NF-kB, MAPK, and NLRP3, exhibit anti-inflammatory and antioxidant effects by modulating the inflammatory signaling pathway [30–33]. Silibinin, which is an extract of milk thistle seed, is an ancient traditional medicine [34,35]. Studies have shown that silibinin targets NF-kB and has anti-inflammatory and anti-cancer effects in several organs [36–39]. However, there is no direct evidence of the therapeutic effects of silibinin in a lung inflammation mouse model induced by V_2O_5. Therefore, in the present study, we investigated the anti-inflammatory and antioxidant effects of silibinin on V_2O_5-induced lung inflammation.

Results

Silibinin increases human lung epithelial cell viability in vitro.

Treatment of inflammatory diseases with natural compounds has several advantages, such as reducing patient treatment costs and side effects. Therefore, we screened in vitro natural compounds that are effective in reducing lung inflammation. First, we measured the viability of human lung epithelial cells (L132) when exposed to V_2O_5 at various times and concentrations. When exposed to V_2O_5, L132 viability showed a tendency to decrease at high concentrations after 24 h and exhibited a significant dose-dependent decrease after 72 h (Fig. 1A). After the cells were treated with 10 μM V_2O_5, various drugs and natural compounds were screened for molecules showing effective anti-inflammatory effects in L132 cells. As a result, cell viability recovered in the experimental group as much as the control group when silibinin was treated for 96 h (Fig. 1B).

Effects of silibinin treatment on lung inflammation caused by V_2O_5 inhalation.

It is known that the infiltration of inflammatory cells in lung tissue increases when an inflammatory response occurs [24]. Therefore, we performed H&E staining on the collected lung tissue for histological analysis. In the V_2O_5 group, extensive infiltration of inflammatory cells was observed in the bronchoalveolar of the lung tissue. In contrast, the silibinin-treated group exhibited a significant decrease in inflammatory cell infiltration compared with the V_2O_5 group (Figure 2A). Furthermore, the results of the bronchial wall thickness measurement also showed a remarkable increase in the V_2O_5 group, and a decrease when treated with silibinin (Figure 2B). Additionally, the H score significantly increased in the V_2O_5 group compared with that of the control group, whereas it significantly decreased in the silibinin group compared with that of the V_2O_5 group (Figure 2C).

Silibinin decreases the V2O5-induced increase in neutrophils and WBC in whole blood.

During an inflammatory reaction, WBCs increase in the body to resist pathogens and thereby activate an immune response [35]. We obtained whole blood from V2O5-induced inflammatory mice and determined the WBC cell number. Compared with the control groups, the group exposed to V2O5 had significantly increased numbers of WBC, neutrophils, lymphocytes, and eosinophils. In contrast, the 50 mg/kg silibinin-treated group showed a significantly decreased inflammatory cell count, including WBC, neutrophils, and eosinophils. However, the 100 mg/kg silibinin-treated group showed a significant decrease in inflammatory cells, but the effect was not as pronounced as the 50 mg/kg silibinin group (Fig. 3A–D).

Silibinin decreases the levels of inflammatory cytokines in V2O5-induced lung injury mice.

Next, we used real-time PCR to measure the expression of inflammatory cytokines. When an inflammatory reaction occurs, inflammatory cytokines are released following activation of upstream signaling pathways, and the inflammatory reaction is triggered [25,26]]. We measured the expression of TNF-α, IL-6, and IL-1β mRNAs, which are known as inflammatory cytokines by real-time PCR. The levels of these cytokines significantly increased in the V2O5 group. However, when silibinin was administered, the expression levels were significantly decreased in a dose-dependent manner (Figure 4A–C).

Effects of silibinin on TNF-α and IL-1β protein levels.

To confirm the results of real-time PCR analysis, we performed a western blot analysis on TNF-α and IL-1β. V2O5-treated mice showed a noticeable increase of TNF-α and IL-1β expression compared with that in control mice. In contrast, 50 mg/kg silibinin-treated mice exhibited a decrease in TNF-α and IL-1β expression compared with V2O5-treated mice whereas 100 mg/kg silibinin-treated mice had no effect on expression (Figs. 5A–C).

Effects of silibinin on the expression of TLR4, NLRP3, NF-kB, and MAPK expression. The previous results showed that the expression of pro-inflammatory cytokines was increased at the protein level. We confirmed that this occurred through TLR4, MAPK, NF-kB, and NLRP3, the upstream signaling pathways that mediate expression. The V2O5-treated mice exhibited a significant increase in the activation of TLR4 and NLRP3, which are downstream signals, compared with the control mice. Also, a significant increase in pp65, which plays an important role in inflammation mediation, was observed. However, 50 mg/kg silibinin-treated mice showed a decrease in TLR4, NLRP3, and pp65 expression compared with V2O5-treated mice, whereas 100 mg/kg silibinin-treated mice exhibited no effect on expression (Figure 6A). Compared with the control mice, V2O5-treated mice showed increased levels of pERK, pJNK, and p38. However, these increases following V2O5 exposure were reduced by 50 mg/kg silibinin treatment, whereas the 100 mg/kg dose had no effect (Figure 6B).

Effects of silibinin on the expression of NLRP3 in lung tissue.

The NLRP3 inflammasome is activated during the inflammatory process and causes the expression of inflammatory cytokines, such as IL-1β. Hence, we performed the experiment with the expectation that silibinin would reduce inflammation by down-regulating this signaling pathways. We confirmed the expression level of NLRP3, which is an important component of the inflammatory response, by IHC staining in lung tissue. The V2O5-treated mice showed an increase in NLRP3 expression in lung tissue compared with the control mice. However, compared with V2O5-treated mice, silibinin-treated mice showed a decrease in NLRP3 expression in a dose-dependent manner (Figure 7A). This suggests that silibinin is effective at relieving lung inflammation by significantly reducing the expression of NLRP3 in lung tissue.

Discussion

Air pollution is regarded as a major global problem, in part, because of the increase in PMs. Among the various components, V2O5 causes changes in various organs and induces an inflammatory response specifically in the lungs [40]. In the present study, we used a V2O5-induced lung injury mouse model to evaluate the therapeutic effect of silibinin, a natural compound. Silibinin alleviated pulmonary inflammation by down-regulating the activities of TLR4/MAPK/NF-kB and the NLRP3 inflammasome in vivo. Most importantly, this study confirmed toxicity by whole-body inhalation of PM components and describes a useful model for studying the preventive and therapeutic effects of natural compounds.

The in vitro results suggested that silibinin inhibits the inflammatory response caused by V2O5 (Fig. 1). Silibinin was effective among various compounds in relieving V2O5-induced normal lung epithelial cells. The effects of silibinin treatment were confirmed in a mouse model of V2O5-induced lung inflammation. We also found that silibinin treatment significantly reduced the invasion of inflammatory cells (Fig. 2). This indicated that silibinin alleviated the inflammatory response in a mouse model of lung injury. Next, we analyzed whole blood to determine the change in WBC count during the inflammatory response. These results showed that silibinin exhibited a significant decrease in WBC count in the mouse model of lung injury (Fig. 3). In addition, 50 mg/kg silibinin was more effective than the 100 mg/kg concentration. This suggests that silibinin is effective at reducing WBC without using it at a high concentration. We measured the expression of inflammatory cytokines by real-time PCR to identify molecular changes caused by silibinin (Fig. 4). The results showed that silibinin significantly reduced the mRNA levels of the pro-inflammatory cytokines, TNF-α, IL-6, and IL-1β. We investigated the protein expression TNF-α and IL-1β, which are representative pro-inflammatory cytokines and confirmed that silibinin at 50 mg/kg significantly reduced the expression of these pro-inflammatory cytokines (Fig. 5).

Previous studies have shown that various signaling pathway are involved in the inflammatory response induced by PM [24,41]. Among them, the MAPK and NF-kB signaling pathways are known to contribute to inflammation [28,42–44]. In addition, TLR4 plays an important role in initiating the innate immune response and causes chronic and acute inflammation [45]. The NLRP3 inflammasome is activated during the

inflammatory process and results in the expression of inflammatory cytokines, such as IL-1β [46]. Hence, we performed the experiment with the expectation that silibinin would relieve inflammation by down-regulating the signaling pathway activity.

Our results indicated that the expression of TLR4/MAPK/NFkB/NLRP3 was upregulated in the V2O5-treated group and the activated signal was down-regulated following silibinin administration. This suggests that silibinin regulates inflammation by down-regulating TLR4/MAPK/NFkB/NLRP3 signaling. Finally, we investigated the level of NLRP3 expression in lung tissue. The results indicated that silibinin decreased NLRP3 expression and exhibited a therapeutic effect on the inflammatory response.

Methods

Reagents.

V2O5 (pure 98%, 181.88 MW, CAS #: 1314-62-1) and silibinin (pure 98%, 482.44 MW, CAS #: 22888-70-6) were purchased from Sigma Aldrich. Gefitinib and imatinib (pure 100%, 589.7 MW, CAS #: 13166, 13139) were purchased from Cayman Chemical (Ann Arbor, MI, USA). 6-shogaol was purchased from Chengdu Biopurify (PS010913, Chengdu Push Biotechnology Co, Ltd, China). This research was confirmed that all experiments were performed in accordance with ARRIVE guidelines.

Cell culture.

The human lung embryo cell line, L132, was purchased from the Korea Cell Line Bank (Seoul, Korea). Cells were maintained at 37°C in a humidified atmosphere containing 5% CO2 in RPMI 1640 supplemented with 10% fetal bovine serum (Gibco) and 1% antibiotics.

Cell viability assay.

Cell were seeded into 96-well plates (1 × 103 cells/well) and allowed to attach overnight. They were then treated with various concentrations of compounds or dimethyl sulfoxide for 0, 24, 48, 72, and 96 h. Cells were treated with various concentrations (1, 2, 5, 10, and 15 μM) of V2O5 and incubated at 37°C for 1 h. Subsequently, 10 μl CCK-8 reagent was added to each well and the cells were incubated for an additional 2 h. The absorbance was measured at 450 nm using a microplate reader. When the compounds was evaluated, the cells were treated in the same manner. The compounds were used at a concentration of 20 μM 1 h before V2O5 treatment.

Animals.

Eight-week-old male BALB/c mice were maintained in an environment a humidity of 50 ± 10%, a 12 h light/dark cycle, and a temperature of 22 ± 2°C. The mice were provided with tap water and weighed weekly. The Animal Testing Ethics Committee of Kyungpook National University approved this study for animal experiments (approval no. 2019-0056).

Establishment of lung injury mice.

Mice were randomized in to four groups (6 mice per group): (1) control; (2) V2O5; (3) V2O5 + silibinin 50 mg/kg; (4) V2O5 + silibinin 100 mg/kg. Silibinin was dissolved in 100 μl of distilled water at a dose of 50 mg/kg (low dose) and 100 mg/kg (high dose). Mice were pretreated with silibinin 50 mg/kg; 100 mg/kg in 100 μl by oral administration, 1 h before V2O5 exposure. The mice were placed in a whole-body inhalation chamber (Gaon bio, Yongin, Republic of Korea), where they were exposed to particulate aerosols of V2O5 concentration of either 0 (control) or 4 mg/m3 (V2O5 group, silibinin 50 mg/kg group, silibinin 100 mg/kg group) for 6 h per day, 3 days per week for 8 weeks [20,47]. The mice were sacrificed after the final exposure by cervical dislocation.

Whole blood analysis.

Immediately after sacrifice, whole blood was obtained from the mice and analysed using an ADVIA 120 Hematology system (Korea Polytech College, Nonsan, Korea). Next, cell number analysis of white blood cells (WBC), neutrophils, lymphocytes, and eosinophils were performed.

Histological analysis.

Mouse lung tissues were fixed with 4% formaldehyde, paraffin-embedded, and cut into 4-μm sections. The sections were stained with hematoxylin–eosin (H&E). Each section was observed using a light microscope (Olympus BX43, Olympus, Tokyo, Japan) to estimate inflammatory cell infiltration. Furthermore, the bronchial thickness in lung tissue and H scoring was determined by skilled researchers. The H score was considered 5 points if the intensity of inflammation was severe and 1 point if inflammation was weak.

RNA extraction and real-time PCR.

Total RNA was isolated from lung tissues using TRIzol reagent. Total RNA was converted to cDNA using the PrimeScript™ 1st strand cDNA synthesis kit (6110, Takara, China). For PCR amplification, the following primers were used: mouse β-actin forward, 5'-GGC TCT TTT CCA GCC TTC CT-3' and reverse, 5'-GTC TTT ACG GAT GTC AAC GTC ACA-3'; IL-1β forward, 5'-CCC CAG GGC ATG TTA AGG A-3', and reverse, 5'-TGA CCC TGA GCG ACC TGT CT-3'; IL-6 forward, 5'-GTT GTG CAA TGG CAA TTC TGA-3', and reverse, 5'-TTG GTA GCA TCC ATC ATT TCT TTG-3'; TNF-α forward, 5'-AGG ACC CAG TGT GGG AAG CT-3', and reverse, 5'-AAA GAG Prime Script GCA ACA AGG TAG AGA-3'. The PCR reaction mixture contained 8 μl cDNA, 10 μl Power SYBR Green PCR Master Mix (4367659, Applied Biosystems, UK), 1 μl 0.2 pmol forward primer, and 1 μl 0.2 pmol reverse primer. The Applied Biosystems real-time PCR program consisted of a holding stage at 95°C for 10 min, followed by 40 cycles of cycling at 95°C for 15 s, 60°C for 1 min, followed by a melt curve. The relative expression of IL-1β, IL-6, and TNF-α mRNA were normalized to that of β-actin mRNA.

Western blot analysis.

Lung tissues were homogenized in tissue lysis buffer (Intron Biotechnology, Korea). Protein concentration was determined using the BCA Protein Assay reagent (Thermo Scientific) according to the manufacturer's instructions. Equal amounts of protein lysate was separated by SDS-PAGE and transferred to polyvinylidene difluoride membranes. The membranes were incubated overnight with primary antibodies at 4°C. The following primary antibodies and dilutions were used: TNF-α, IL-1β, phospho-p38, total p38, phospho-JNK, total JNK, phospho-ERK1/2, total ERK1/2, phosphor-p65, total p65, NLRP3 (1:1000 dilution; Cell signaling Technology, MA, USA), SOD1, and SOD2 (1:1000 dilution; Santacruz Biotechnology, CA, USA). Subsequently, the membranes were incubated with corresponding secondary antibodies for 1 h at room temperature. Immunoblots were visualized using ECL detection kit (GE Healthcare, Seoul, Korea) by Imagequant™ LAS 500 (GE Healthcare).

Immunohistochemical analysis (IHC).

NLRP3 proteins in lung tissues were examined with immunohistochemical (IHC) staining. The samples were fixed with paraformaldehyde at 4°T for 4 h, washed with phosphate-buffered saline containing 20% sucrose for 4 h, embedded and cut into 4-μm-thick sections on acid pretreated slides. After dewaxing, blocking endogenous peroxidase, and repairing the antigen, the lung tissue sections were incubated with anti-rabbit NLRP3 antibodies (1:200 dilution) at 4°C overnight, followed by incubation with HRP-labeled Goat Anti-Mouse IgG (H + L) as a secondary antibody (1:100 dilution) at 37°C for 30 min. The results were observed under a light microscope.

Statistical analysis.

All results are expressed as the means ± standard deviation (SD) from at least three independent experiments. All analyses were performed using SPSS software (IBM SPSS Statistics 26.0). Normality tests were performed with Kolmogorov-Smirnov and Shapiro-Wilk test ($P > 0.05$). Statistical significance between experimental groups was determined using one-way ANOVA for pair-wise comparisons with Dunnett's test. $P < 0.05$ was considered to indicate a statistically significant difference.

Declarations

Author contributions

MK and JKY designed and supervised experiment. EK and HBI designed and performed experiment. HJK, HK, NEC and JK analyzed and interpretated data. HBI, EK, YS and SJ wrote manuscript. SHK, EJL, DY, WSK and ZYR reviewed manuscript. All authors reviewed and approved the final manuscript.

Competing interests

The authors declare that they have no competing interests.

Data availability

The datasets used and/or analysed during the current study available from the corresponding author on reasonable request.

Ethics declarations

The Animal Testing Ethics Committee of Kyungpook National University approved this study for animal experiments (approval no. 2019-0056).

References

1. Bascom, R.*et al.* Health effects of outdoor air pollution. **153**, 477-498 (1996).
2. He, C., Pan, F. & Yan, Y. Is economic transition harmful to China's urban environment? Evidence from industrial air pollution in Chinese cities. *Urban Studies* **49**, 1767-1790 (2012).
3. Jerrett, M., Buzzelli, M., Burnett, R. T. & DeLuca, P. F. Particulate air pollution, social confounders, and mortality in small areas of an industrial city. *Social science medicine* **60**, 2845-2863 (2005).
4. Janssen, N. A., Schwartz, J., Zanobetti, A. & Suh, H. H. Air conditioning and source-specific particles as modifiers of the effect of PM (10) on hospital admissions for heart and lung disease. *J Environmental health perspectives* **110**, 43-49 (2002).
5. Afsar, B.*et al.* Air pollution and kidney disease: review of current evidence. *Clinical Kidney Journal* **12**, 19-32 (2019).
6. Beamish, L. A., Osornio-Vargas, A. R. & Wine, E. Air pollution: An environmental factor contributing to intestinal disease. *Journal of Crohn's Colitis* **5**, 279-286 (2011).
7. Calderón-Garcidueñas, L.*et al.* Long-term air pollution exposure is associated with neuroinflammation, an altered innate immune response, disruption of the blood-brain barrier, ultrafine particulate deposition, and accumulation of amyloid β-42 and α-synuclein in children and young adults. *Toxicologic pathology* **36**, 289-310 (2008).
8. Valavanidis, A., Fiotakis, K. & Vlachogianni, T. Airborne particulate matter and human health: toxicological assessment and importance of size and composition of particles for oxidative damage and carcinogenic mechanisms. *Journal of Environmental Science Health, Part C* **26**, 339-362 (2008).
9. Chen, H., Shi-Jin, S. & Jian-Xin, W. Study on combustion characteristics and PM emission of diesel engines using ester–ethanol–diesel blended fuels. *Proceedings of the Combustion institute* **31**, 2981-2989 (2007).
10. Hopke, P. K.*et al.* PM source apportionment and health effects: 1. Intercomparison of source apportionment results. *Journal of exposure science environmental epidemiology* **16**, 275-286 (2006).
11. Bae, J.-W.*et al.* Vanadium adversely affects sperm motility and capacitation status via protein kinase A activity and tyrosine phosphorylation. *Reproductive Toxicology* **96**, 195-201 (2020).
12. Pinon-Zarate, G.*et al.* Vanadium pentoxide inhalation provokes germinal center hyperplasia and suppressed humoral immune responses. *Journal of immunotoxicology* **5**, 115-122 (2008).

13. Cooper, R. G. Vanadium pentoxide inhalation.*Indian journal of occupational environmental medicine* **11**, 97 (2007).
14. Kiviluoto, M. Observations on the lungs of vanadium workers. *Occupational Environmental Medicine* **37**, 363-366 (1980).
15. Knecht, E. A., Moorman, W. J., Clark, J. C., Lynch, D. W. & Lewis, T. R. Pulmonary effects of acute vanadium pentoxide inhalation in monkeys. *American Review of Respiratory Disease* **132**, 1181-1185 (1985).
16. Fortoul, T.*et al.* Inhalation of vanadium pentoxide and its toxic effects in a mouse model. *Inorganica Chimica Acta* **420**, 8-15 (2014).
17. Soares, S., Martins, H., Gutiérrez-Merino, C. & Aureliano, M. Vanadium and cadmium in vivo effects in teleost cardiac muscle: metal accumulation and oxidative stress markers. *Comparative Biochemistry Physiology Part C: Toxicology Pharmacology* **147**, 168-178 (2008).
18. Levy, B. S., Hoffman, L. & Gottsegen, S. Boilermakers' bronchitis. Respiratory tract irritation associated with vanadium pentoxide exposure during oil-to-coal conversion of a power plant. *Journal of occupational medicine.: official publication of the Industrial Medical Association* **26**, 567-570 (1984).
19. Rondini, E. A., Walters, D. M. & Bauer, A. K. Vanadium pentoxide induces pulmonary inflammation and tumor promotion in a strain-dependent manner. *Particle fibre toxicology* **7**, 9 (2010).
20. Ress, N.*et al.* Carcinogenicity of inhaled vanadium pentoxide in F344/N rats and B6C3F1 mice.*Toxicological Sciences* **74**, 287-296 (2003).
21. González-Villalva, A.*et al.* Thrombocytosis induced in mice after subacute and subchronic V2O5 inhalation. *Toxicology industrial health* **22**, 113-116 (2006).
22. Rodríguez-Lara, V., Morales-Rivero, A., Rivera-Cambas, A. M. & Fortoul, T. I. Vanadium inhalation induces actin changes in mice testicular cells. *Toxicology industrial health* **32**, 367-374 (2016).
23. Knecht, E. A.*et al.* Pulmonary reactivity to vanadium pentoxide following subchronic inhalation exposure in a non-human primate animal model. *Journal of applied toxicology* **12**, 427-434 (1992).
24. Wang, J.*et al.* Urban particulate matter triggers lung inflammation via the ROS-MAPK-NF-κB signaling pathway. *J Thorac Dis* **9**, 4398-4412, doi:10.21037/jtd.2017.09.135 (2017).
25. Lai, J. L.*et al.* Indirubin Inhibits LPS-Induced Inflammation via TLR4 Abrogation Mediated by the NF-kB and MAPK Signaling Pathways. *Inflammation* **40**, 1-12, doi:10.1007/s10753-016-0447-7 (2017).
26. Ye, J.*et al.* Polydatin inhibits mast cell-mediated allergic inflammation by targeting PI3K/Akt, MAPK, NF-κB and Nrf2/HO-1 pathways. *Sci Rep* **7**, 11895, doi:10.1038/s41598-017-12252-3 (2017).
27. Pahl, H. L. Activators and target genes of Rel/NF-kappaB transcription factors. *Oncogene* **18**, 6853-6866, doi:10.1038/sj.onc.1203239 (1999).
28. Wang, J.*et al.* Anti-inflammatory effects of apigenin in lipopolysaccharide-induced inflammatory in acute lung injury by suppressing COX-2 and NF-kB pathway. *Inflammation* **37**, 2085-2090 (2014).

29. Goodman, R. B., Pugin, J., Lee, J. S. & Matthay, M. A. Cytokine-mediated inflammation in acute lung injury. *Cytokine growth factor reviews* **14**, 523-535 (2003).
30. Yang, H., Lv, H., Li, H., Ci, X. & Peng, L. Oridonin protects LPS-induced acute lung injury by modulating Nrf2-mediated oxidative stress and Nrf2-independent NLRP3 and NF-κB pathways. *Cell Commun Signal* **17**, 62, doi:10.1186/s12964-019-0366-y (2019).
31. Tanaka, T., Yasui, Y., Ishigamori-Suzuki, R. & Oyama, T. Citrus compounds inhibit inflammation-and obesity-related colon carcinogenesis in mice. *Nutrition Cancer* **60**, 70-80 (2008).
32. Pan, M.-H., Lai, C.-S., Dushenkov, S. & Ho, C.-T. Modulation of inflammatory genes by natural dietary bioactive compounds.*Journal of agricultural food chemistry* **57**, 4467-4477 (2009).
33. Hošek, J.*et al.* Natural compound cudraflavone B shows promising anti-inflammatory properties in vitro. *Journal of Natural Products* **74**, 614-619 (2011).
34. Singh, R. P. & Agarwal, R. Cosmeceuticals and silibinin. *Clinics in dermatology* **27**, 479-484 (2009).
35. Park, J. W.*et al.* Silibinin inhibits neutrophilic inflammation and mucus secretion induced by cigarette smoke via suppression of ERK-SP1 pathway. *Phytotherapy Research* **30**, 1926-1936 (2016).
36. Salamone, F.*et al.* Silibinin modulates lipid homeostasis and inhibits nuclear factor kappa B activation in experimental nonalcoholic steatohepatitis. *Translational Research* **159**, 477-486 (2012).
37. Chen, P. N., Hsieh, Y. S., Chiou, H. L. & Chu, S. C. Silibinin inhibits cell invasion through inactivation of both PI3K-Akt and MAPK signaling pathways. *Chem Biol Interact* **156**, 141-150, doi:10.1016/j.cbi.2005.08.005 (2005).
38. Lee, S. O.*et al.* Silibinin suppresses PMA-induced MMP-9 expression by blocking the AP-1 activation via MAPK signaling pathways in MCF-7 human breast carcinoma cells. *Biochem Biophys Res Commun* **354**, 165-171, doi:10.1016/j.bbrc.2006.12.181 (2007).
39. Tian, L., Li, W. & Wang, T. Therapeutic effects of silibinin on LPS-induced acute lung injury by inhibiting NLRP3 and NF-κB signaling pathways. *Microb Pathog* **108**, 104-108, doi:10.1016/j.micpath.2017.05.011 (2017).
40. Rondini, E. A., Walters, D. M., Bauer, A. K. J. P. & toxicology, f. Vanadium pentoxide induces pulmonary inflammation and tumor promotion in a strain-dependent manner. **7**, 9 (2010).
41. Yang, H.*et al.* Oridonin attenuates carrageenan-induced pleurisy via activation of the KEAP-1/Nrf2 pathway and inhibition of the TXNIP/NLRP3 and NF-κB pathway in mice. **28**, 513-523 (2020).
42. Huang, P., Han, J., Hui, L. J. P. & cell. MAPK signaling in inflammation-associated cancer development. **1**, 218-226 (2010).
43. Underwood, D. C.*et al.* SB 239063, a p38 MAPK inhibitor, reduces neutrophilia, inflammatory cytokines, MMP-9, and fibrosis in lung. **279**, L895-L902 (2000).
44. Nennig, S., Schank, J. J. A. & Alcoholism. The role of NFkB in drug addiction: beyond inflammation. **52**, 172-179 (2017).
45. Kuzmich, N. N.*et al.* TLR4 signaling pathway modulators as potential therapeutics in inflammation and sepsis. **5**, 34 (2017).

46. Grailer, J. J.*et al.* Critical role for the NLRP3 inflammasome during acute lung injury. **192**, 5974-5983 (2014).
47. Program, N. T. NTP toxicology and carcinogensis studies of vanadium pentoxide (CAS No. 1314-62-1) in F344/N rats and B6C3F1 mice (inhalation). *National Toxicology Program technical report series*, 1-343 (2002).

Figures

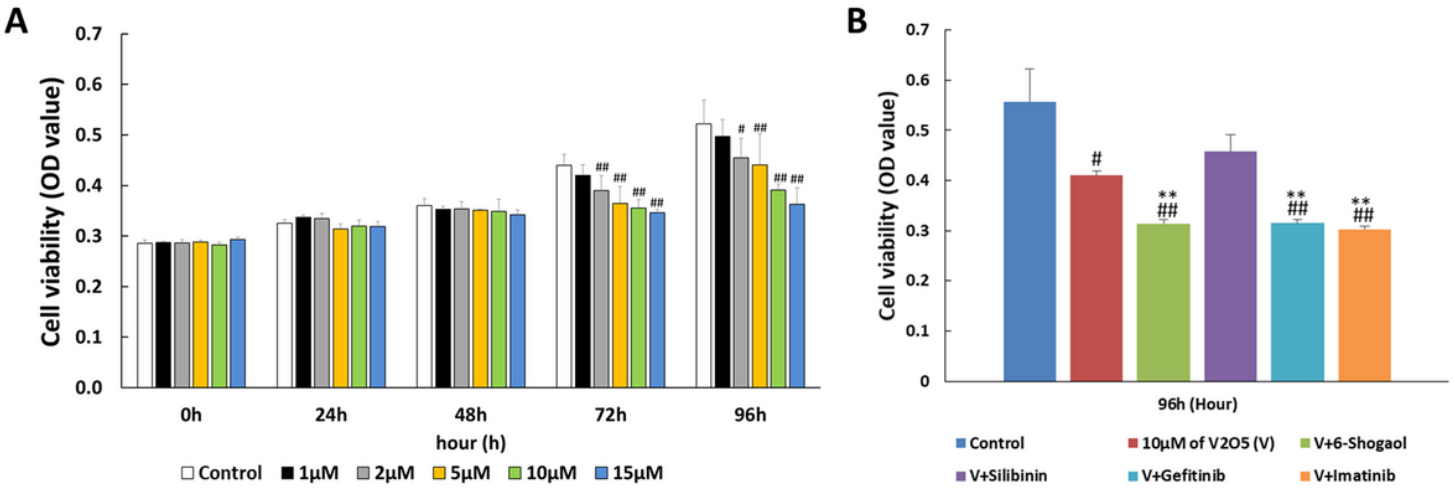

Figure 1

Silibinin effectively increased cell viability in V_2O_5-treated L132 cells. (A) The cells (1×10^3 cells/well) were treated with V_2O_5 at various concentrations (1, 2, 5, 10, and 15 μM of V_2O_5). (B) The cells were treated 6-shogaol, silibinin, gefitibib, gossy peptin and imatinib with 10 μM of V_2O_5. Cell viability was measured by CCK-8 assay. The cell viability is expressed as an OD value (mean ± SD). #P < 0.05, ##P < 0.01, and ###P < 0.005 as compared with the control group. *P < 0.05, **P < 0.01, and ***P < 0.005 as compared with the V_2O_5 group.

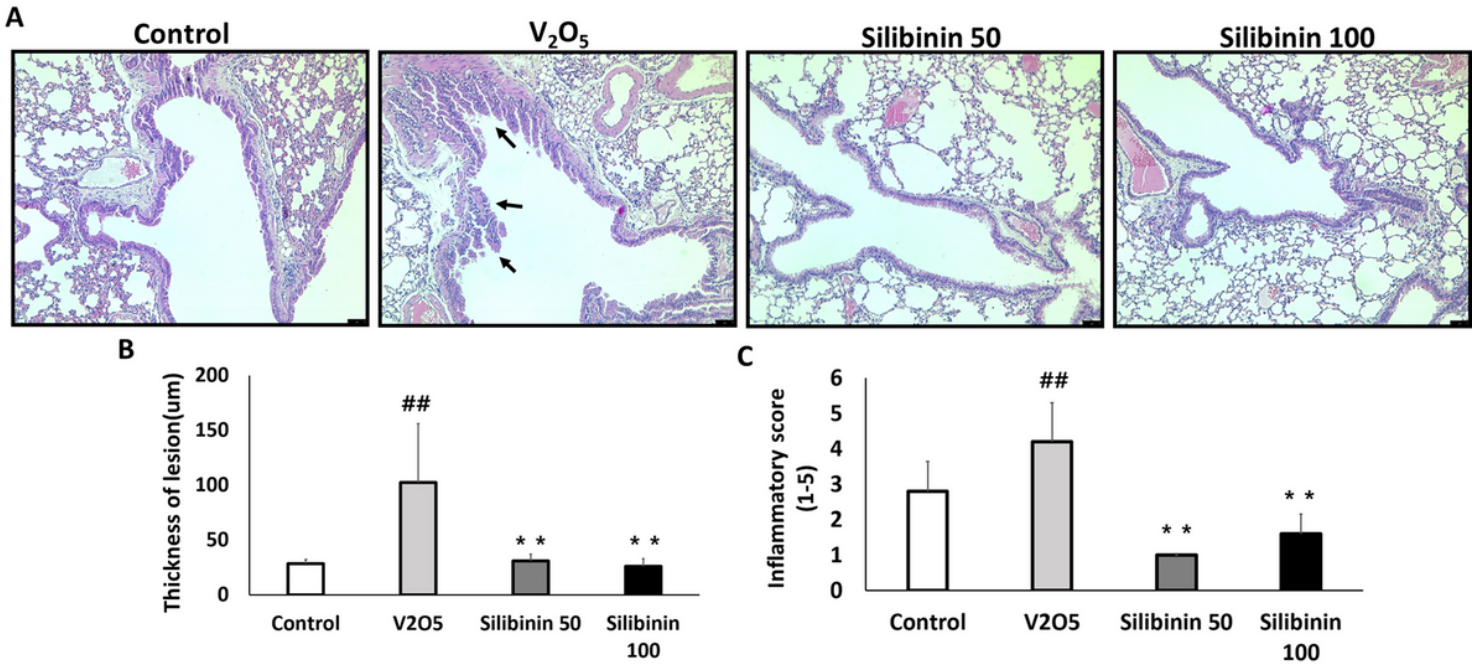

Figure 2

Effects of silibinin on inflammatory cell infiltration and bronchoalveolar inflammation in lung tissues. The control group was treated with saline only; V2O5 mice were treated with V2O5 by whole-body inhalation; Silibinin 50 and 100 mice were treated with silibinin (50 or 100 mg/kg) and V2O5 whole-body inhalation. (A) Lung tissues were stained with hematoxylin and eosin (X100). The black arrows indicate epithelial cells in the lung tissue. (B) The thickness of the bronchoalveolar in the lung tissues were calculated as the average of the measures three times in four directions. (C) The inflammatory score was calculated as an average of the response values. Data are shown as the mean ± SD (n = 6). #P < 0.05, ##P < 0.01, and ###P < 0.005 as compared with the control group. *P < 0.05, **P < 0.01, and ***P < 0.005 as compared with the V2O5 group.

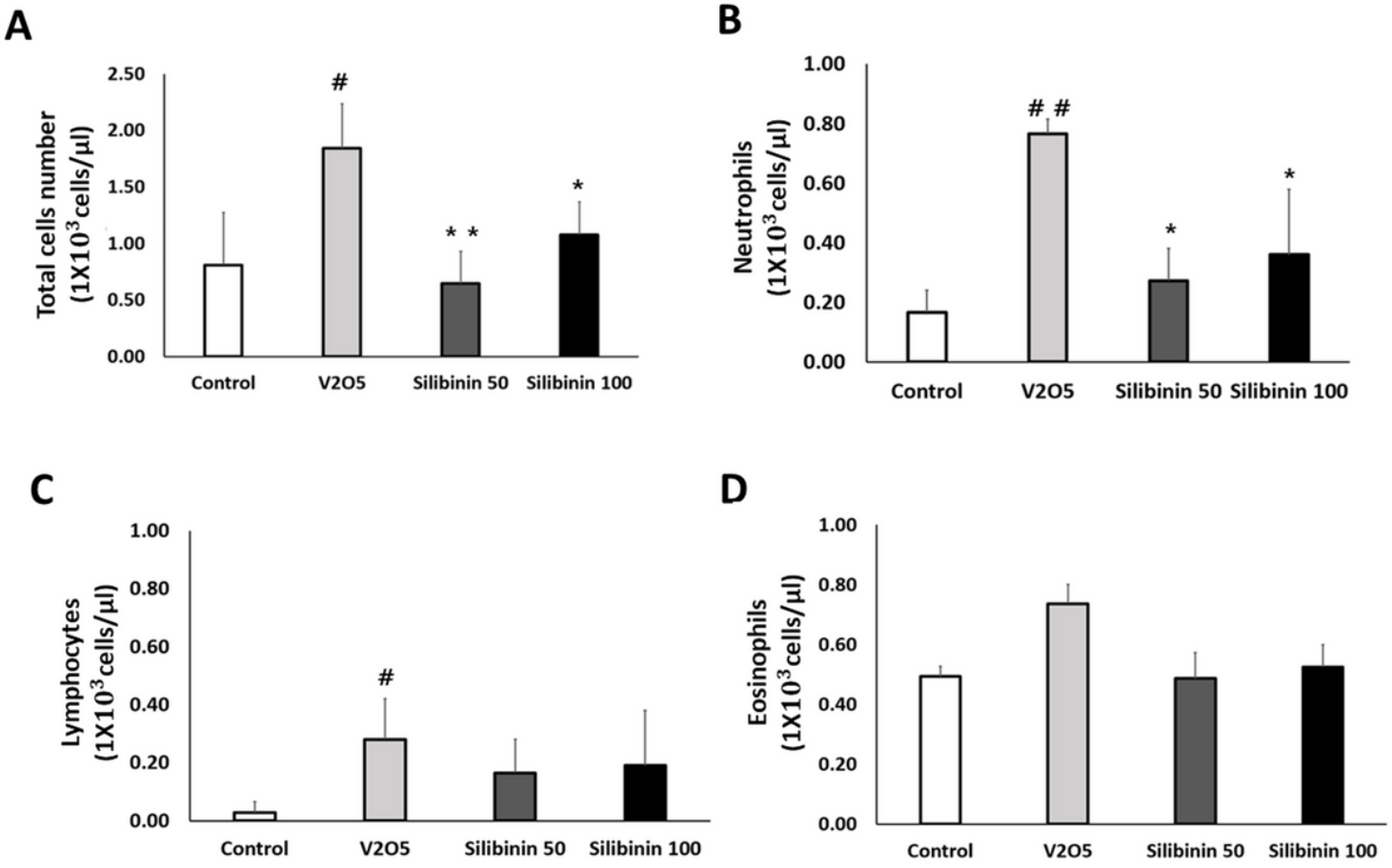

Figure 3

Silibinin effectively reduces the number of inflammatory cells in the blood. Whole blood was immediately obtained from the abdominal aorta after sacrifice, and total cell count and differential cell count was determined using the ADVIA 120 Hematology system. White blood cells were classified as (A) total cells, (B) neutrophils, (C) lymphocytes, and (D) eosinophils. Data are shown as the mean ±SEM (n=6). Data are shown as the mean ± SD (n = 6). #P < 0.05, ##P < 0.01, and ###P < 0.005 as compared with the control group. *P < 0.05, **P < 0.01, and ***P < 0.005 as compared with the V2O5 group.

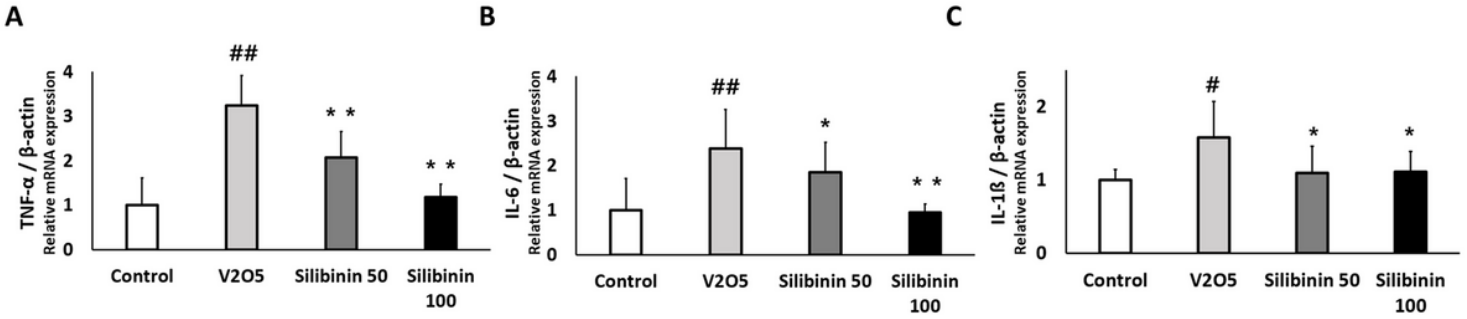

Figure 4

Effects of silibinin on the expression of pro-inflammatory cytokine mRNAs in lung tissue. Total RNA was isolated form lung tissues. (A) TNF-α, (B) IL-6, and (C) IL-1β mRNA were measured by real-time PCR The relative levels of mRNA were calculated based on β-actin mRNA levels. Data are shown as the mean ± SD (n = 6). #P < 0.05, ##P < 0.01, and ###P < 0.005 as compared with the control group. *P < 0.05, **P < 0.01, and ***P < 0.005 as compared with the V2O5 group.

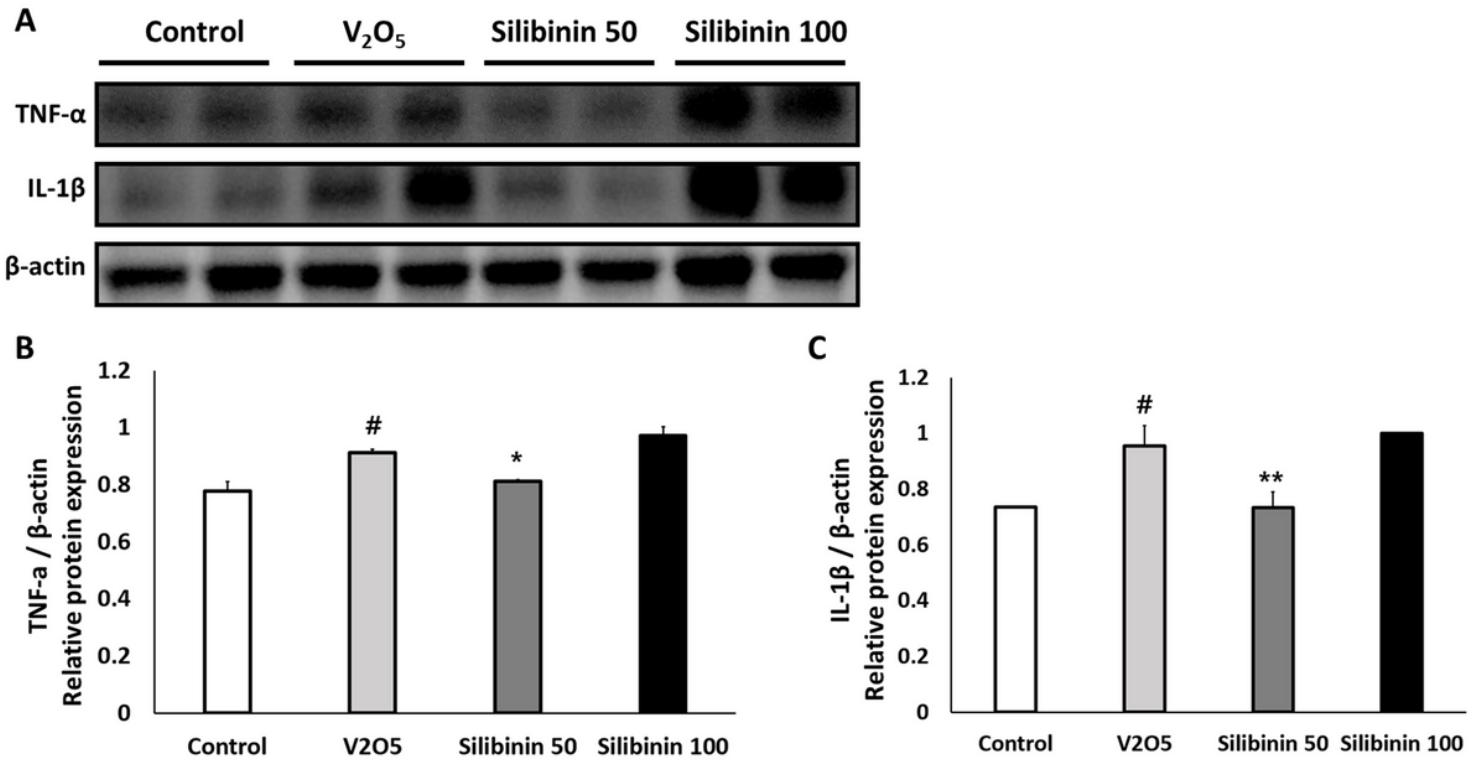

Figure 5

Silibinin effectively reduced protein expression levels of inflammatory cytokines in lung tissue. Control mice treated with saline only; V2O5, mice treated with V2O5 whole-body inhalation; Silibinin 50 and 100, mice treated with silibinin (50 and 100 mg/kg) + V2O5 whole-body inhalation (A–C). The relative levels of protein expression were calculated based on β-actin protein expression levels in lung tissue. Data are shown as mean ± SD (n = 6). #P < 0.05, ##P < 0.01, and ###P < 0.005 as compared with the control group. *P < 0.05, **P < 0.01, and ***P < 0.005 as compared with the V2O5 group.

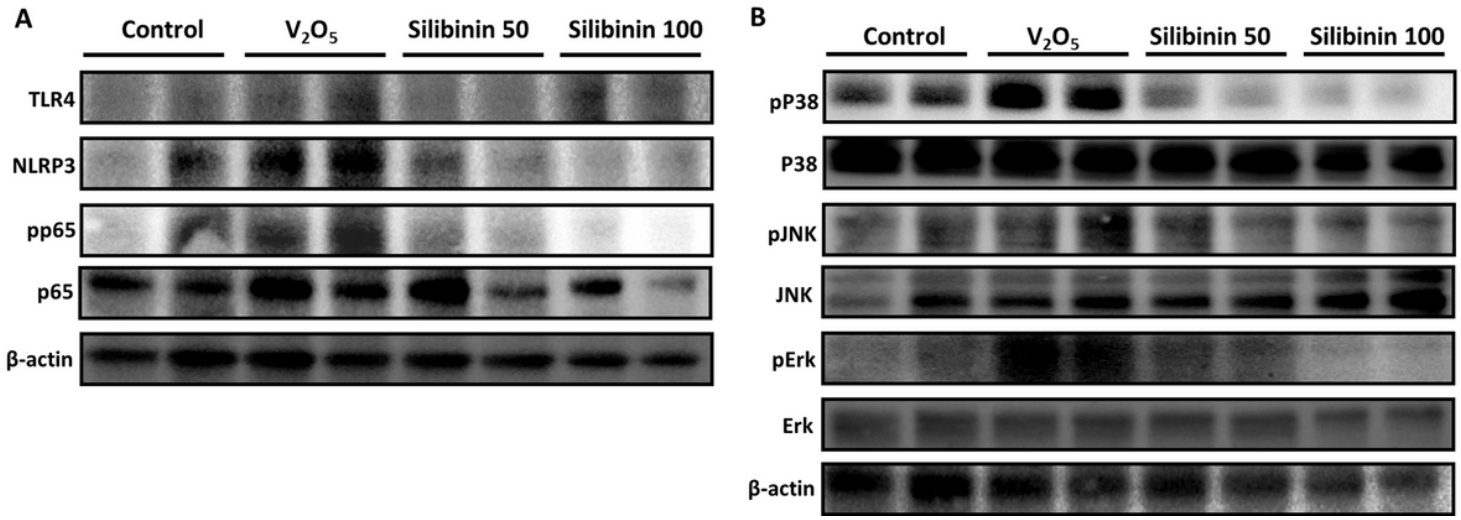

Figure 6

Silibinin effectively reduced the protein expression of MAPK signaling pathway components in lung tissue. Control mice treated with saline only; V2O5, mice treated with V2O5 whole-body inhalation; Silibinin 50 and 100, mice treated with silibinin (50 and 100 mg/kg) + V2O5 whole-body inhalation. Protein expression levels of TLR4, NLRP3, and NF-kB signal members, pp65 and p65 (A). Protein expression levels of MAPK signal pathways (pp38, p38, pJNK, JNK, pErk and Erk) (B).

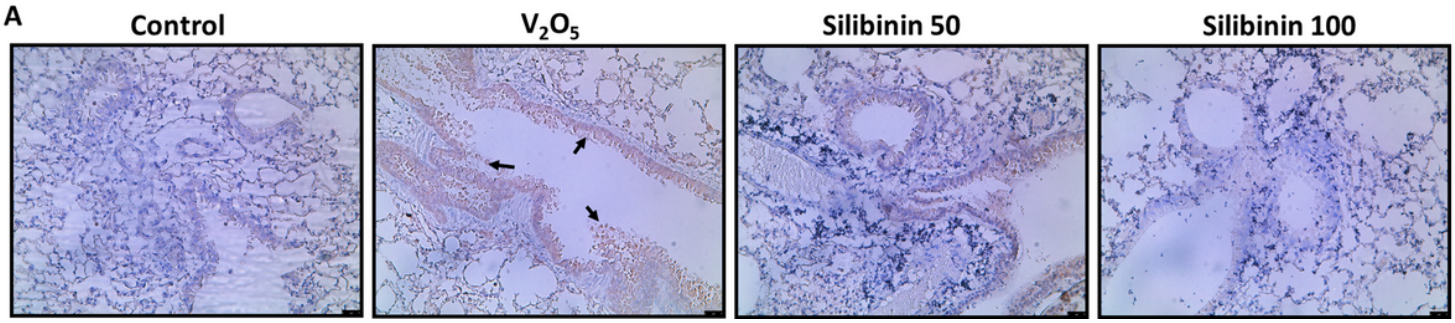

Figure 7

Effect of silibinin treatment on NLRP3 expression in lung tissue. (A) Lung tissues were used for IHC using an anti-NLRP3 antibody. Control mice treated with saline only; V2O5, mice treated with V2O5 whole-body inhalation; Silibinin 50 and 100, mice treated with silibinin (50 and 100 mg/kg) + V2O5 whole-body inhalation. The black arrows indicate where NLRP3 is highly distributed.